



The tumor suppressor FOXO3a mediates the response to EGFR inhibition in glioblastoma cells

Guillem Ramis^{1,2} · Ruth Villalonga-Planells³ · Margalida Serra-Sitjar¹ · Marta Brell⁴ · Silvia Fernández de Mattos^{1,5} · Priam Villalonga^{1,5} 

Accepted: 25 March 2019 / Published online: 13 April 2019
© International Society for Cellular Oncology 2019

Abstract

Purpose Although EGFR activation is a hallmark of glioblastoma (GBM), anti-EGFR therapy has so far not yielded the desired effects. Targeting PI3K/Akt has been proposed as a strategy to increase the cellular sensitivity to EGFR inhibitors. Here we evaluated the contribution of FOXO3a, a key Akt target, in the response of GBM cells to EGFR inhibition.

Methods FOXO3a activation was assessed by immunofluorescence and gene reporter assays, and by evaluating target gene expression using Western blotting and qRT-PCR. Cellular effects were evaluated using cell viability and apoptosis assays, i.e., Annexin V/PI staining and caspase 3/7 activity measurements. Drug synergism was evaluated by performing isobolographic analyses. Gene silencing experiments were performed using stable shRNA transfections.

Results We found that EGFR inhibition in GBM cells led to FOXO3a activation and to transcriptional modulation of its key targets, including repression of the oncogene FOXM1. In addition, we found that specific FOXO3a activation recapitulated the molecular effects of EGFR inhibition, and that the FOXO3a activator trifluoperazine, a FDA-approved antipsychotic agent, reduced GBM cell growth. Subsequent isobolographic analyses of combination experiments indicated that trifluoperazine and erlotinib cooperated synergistically and that their concomitant treatment induced a robust activation of FOXO3a, leading to apoptosis in GBM cells. Using gene silencing, we found that FOXO3a is essential for the response of GBM cells to EGFR inhibition.

Conclusions Our data indicate that FOXO3a activation is a crucial event in the response of GBM cells to EGFR inhibition, suggesting that FOXO3a may serve as an actionable therapeutic target that can be modulated using FDA-approved drugs.

Keywords Glioblastoma · EGFR · Erlotinib · FOXO3a · Trifluoperazine · Phenothiazines

✉ Priam Villalonga
priam.villalonga@uib.es

¹ Cancer Cell Biology Laboratory, Institut Universitari d'Investigació en Ciències de la Salut (IUNICS), Universitat de les Illes Balears, and Institut d'Investigació Sanitària Illes Balears (IdISBa), Ctra. Valldemossa Km 7,5, Palma, Illes Balears, Spain

² Cellomics Unit, Institut Universitari d'Investigació en Ciències de la Salut (IUNICS), Universitat de les Illes Balears, Palma, Illes Balears, Spain

³ Departament de Química, Universitat de les Illes Balears, Palma, Illes Balears, Spain

⁴ Department of Neurosurgery, Hospital Universitari Son Espases, Palma, Illes Balears, Spain

⁵ Departament de Biologia Fonamental i Ciències de la Salut, Universitat de les Illes Balears, Palma, Illes Balears, Spain

1 Introduction

Malignant gliomas are the most common primary brain tumors and represent one of the most lethal human cancers. In their most aggressive manifestation, i.e., grade IV gliomas or glioblastomas (GBMs), patient survival is only 12–15 months. The clinical aggressiveness of GBMs and their dismal prognosis is a consequence of several biological traits, including a highly infiltrative nature, which impairs complete surgical resection, and an increased resistance to radio- and chemotherapy [1–3]. These key biological features, which critically challenge the success of therapeutic intervention, are a consequence of an array of genetic and epigenetic alterations. Recent genomic and transcriptomic analyses have revealed that most of these alterations affect three major signaling pathways: the RTK/Ras/PI3K pathway, the p53-dependent DNA

damage checkpoint response pathway and the pRB-dependent cell cycle restriction point pathway [1, 4]. Within the RTK/Ras/PI3K signaling pathway, the most frequently encountered alterations include hyperactivation of the epidermal growth factor receptor (EGFR) and loss of function of the phosphatase and tensin homolog (PTEN), both contributing to activation of the PI3K/Akt pathway [5]. In 40–50% of GBMs activation of EGFR is achieved through gene amplification, resulting in overexpression [6]. Moreover, almost half of the GBM cases with amplified EGFR also harbor an activating mutation, leading to the expression of a truncated receptor, termed EGFRvIII, which lacks the extracellular domain and is constitutively active [7]. According to its central role in GBM cell biology, EGFR is widely considered as a key therapeutic target, and small molecule EGFR inhibitors such as erlotinib (Tarceva) and gefitinib (Iressa) have been shown to reduce GBM cell proliferation, motility and invasion in vitro [8–10]. However, despite these preclinical data, the clinical benefits achieved so far with EGFR inhibitors as single agents have been very limited and in some cases even controversial due to contradictory data obtained in clinical trials (reviewed in [11]). Consequently, combinatorial therapies with other compounds aimed at increasing GBM sensitivity to EGFR inhibitors, or overcoming resistance, have been proposed [12]. Among these strategies, several efforts have focused on targeting the survival PI3K/Akt/mTOR pathway. In this vein, it has been found that inhibition of EGFR concomitant with PI3K and/or mTOR enhances the efficacy of EGFR inhibition alone [13, 14], and that a dual PI3K/mTOR inhibitor further increases the responsiveness of GBM cells to EGFR inhibitors [15]. As yet, the therapeutic potential of targeting the Akt downstream target FOXO3a has not been explored in malignant gliomas. FOXO3a is one of the best-characterized members of the FOXO subclass of FOX (Forkhead Box) transcription factors that also comprises FOXO1, FOXO4 and FOXO6. FOXO transcription factors share a very similar DNA-binding motif and bind to the same consensus sequence and, as such, are considered to be functionally redundant, although they differ in their tissue distribution [16]. Upon Akt activation, FOXO3a becomes phosphorylated and exported from the nucleus to the cytosol, leading to its functional inactivation as a transcription factor and impairing its function as cell cycle arrest and apoptosis inducer [17]. In agreement with this, FOXO3a has been found to be inactivated by aberrant PI3K/Akt signaling in several human tumors including GBMs, and FOXO3a inactivation has been found to be associated with a poor clinical outcome [18]. Interestingly, several research groups have identified FOXO3a as an attractive therapeutic target in different tumors, and have shown that its functional reactivation may serve a promising therapeutic strategy [19]. Here, we investigated the functional contribution of FOXO3a in the response of GBM cells to EGFR inhibition. Using GBM cell lines and patient-derived primary GBM cells,

we show that EGFR inhibition leads to FOXO3a dephosphorylation, followed by its nuclear translocation and increase in transcriptional activity. Selective activation of FOXO3a using different approaches confirm that FOXO3a reactivation readily elicits in vitro and ex vivo anticancer effects in GBM. Interestingly, we show that pharmacological combination of the FOXO3a activator trifluoperazine with erlotinib induces synergistic effects both in GBM-derived cell lines and in ex vivo primary cultures. In agreement with this observation, we show that trifluoperazine in combination with erlotinib is able to promote apoptosis induction in primary GBM cells, in contrast to the cytostatic effects induced by either compound alone. Finally, we show that FOXO3a silencing in GBM cells dramatically reduces the cellular effects of erlotinib, both alone or in combination with trifluoperazine, indicating that FOXO3a activation is required for mediating EGFR-dependent responses in these cells.

2 Materials and methods

2.1 Cell culture

LN229, U87MG, HS683, T98G, U251 and U373 GBM cells were a gift from Joan Seoane (Institut de Recerca Hospital Universitari Vall d'Hebron, Barcelona, Spain). The U87MG derivative cell line U87 Δ EGFR (a stable transfectant expressing EGFRvIII) was a gift from Isabel Martínez-Lacaci (Hospital Universitario Virgen de la Arrixaca, Murcia, Spain). SKMG-3 GBM cells were a gift from Hans Skovgaard (Rikshospitalet, Oslo, Norway). All cell lines were subconfluently grown and passaged, routinely tested for mycoplasma contamination and subjected to frequent morphological tests and growth curve analyses as quality controls. All cell lines were treated with a prophylactic concentration of 5 μ g/ml PlasmocinTM (InvivoGen, San Diego, CA). Cells were grown in DMEM (Life Technologies, Carlsbad, CA, USA) supplemented with 10% foetal calf serum (FCS, Sigma-Aldrich, St. Louis, MO, USA) in a humidified incubator at 37 °C with 5% CO₂. For primary GBM cell cultures, samples were obtained from patients undergoing surgical treatment at the Department of Neurosurgery of the Hospital Universitari Son Espases (Palma, Spain). The primary cells used in this study were derived from two patients diagnosed with GBM IDH1-wt (W.H.O grade IV). Written informed consent was obtained from all patients by the Hospital's biobank and the study was approved by the local ethical committee (Comitè d'Ètica de la Investigació-Illes Balears, CEI-IB, Ref. N° 3198/16). Tumor fragments were rinsed with Hank's Balanced Salt Solution (HBSS) and mechanically dissociated into ~1–5 mm³ pieces. These pieces were incubated with collagenase I (200 U/ml) in HBSS for 1 h at 37 °C with constant vigorous agitation. The resulting cell suspensions

were washed in complete DMEM culture medium. After centrifugation, the top thin layer of erythrocytes was discarded and pellets were resuspended in culture medium. Cellular suspensions were seeded in 60-mm tissue culture plates and maintained in a humidified incubator at 37 °C with 5% CO₂. Subsequently, confluent cell cultures were split 1 : 2. All experiments were performed before passage 5. For drug treatments, erlotinib (Roche, Basel, Switzerland), psammaplysene A (a gift of Prof. Jon Clardy, Harvard Medical School, Boston, USA) and trifluoperazine (Sigma-Aldrich, St. Louis, MO, USA) were added directly to the media at the indicated concentrations after which the cells were harvested and analysed at the indicated time points.

2.2 Expression vectors, transfection and shRNA-mediated gene silencing

Cells were transfected using Lipofectamine2000 (Life Technologies, Carlsbad, CA, USA) according to the manufacturer's instructions with the following expression plasmids: active FOXO3a (pLPC-FOXO3a-A3, a gift from Eric Lam, Imperial College London, UK), p27^{kip1} promoter vector (pGL3-p27, a gift from Eric Lam, Imperial College London, UK) and FOXO3a-responsive luciferase reporters (pGL3-3xDBE and pGL3-6xDBE, a gift from Wolfgang Link, CNIO, Madrid, Spain). For the generation of FOXO3a-depleted cells, cells were transfected with a FOXO3a shRNA expression vector (pSUPER-FOXO3a, a gift from Eric Lam, Imperial College London, UK), which contains two complementary sequences of 19 nucleotides, TCACTGCATAGTCGATTCA, cloned into the InvivoGen psiRNA plasmid (Autogen Bioclear, Wiltshire, UK). LN229, T98G and U373 cells were reversely transfected in 6-well plates with 2 µg construct using Lipofectamine2000 (Life Technologies, Carlsbad, CA, USA) following the manufacturer's instructions. The transfected cells were left to adhere overnight after which they were carefully washed. After another 24 h selection was started by addition of 0.5 mg/ml zeocin to the growth medium, followed by single cell cloning and expansion for another 2 weeks. The cells were tested for the efficiency of shRNA-mediated silencing using Western blotting.

2.3 Cell viability measurement and IC₅₀ determination

The number of viable cells was determined based on quantification of ATP, which signals the presence of metabolically active cells, using a Cell Titer-Glo luminiscent assay kit (Promega, Madison, WI, USA). Following the manufacturer's instructions, 5×10^3 cells were seeded in 96-well plates, treated 24 h later as indicated, followed by the addition of Cell Titer-Glo reagent. Luminiscent was detected using a multi-well Synergy Mx scanning spectrophotometer (Biotek,

Winooski, VT, USA). For IC₅₀ determination, data obtained from cell viability experiments after dose-response treatments with the indicated drugs were subjected to curve fitting analysis using the GraphPad Prism software (La Jolla, CA, USA).

2.4 Isobolographic analysis

Drug synergy was determined using the isobologram and combination-index (CI) methods, derived from the median-effect principle of Chou and Talalay [20]. Combinations with CI > 1 are considered as antagonistic, those with CI = 1 as additive, and those with CI < 1 as synergistic. Data obtained from cell viability experiments with the indicated fixed-dose drug combinations were subjected to curve fitting analysis using GraphPad Prism software (La Jolla, CA, USA) to determine the IC₅₀ values of each combination represented on the isobologram.

2.5 Caspase activity assay

Enzymatic activity of effector caspases was determined by measurement of caspases-3 and -7 activities using a luminometric Caspase-Glo 3/7 assay (Promega, Madison, WI, USA) according to the manufacturer's protocol in conjunction with a Synergy HT multi-detection microplate reader (Bio-Tek, Winooski, VT, USA).

2.6 Luciferase reporter assay

For reporter assays, the activity of both *Firefly* and *Renilla* luciferase in cell lysates was measured using a Dual-luciferase reporter assay system (Promega, Madison, WI, USA). The assays were performed according to the manufacturer's recommendations. For FOXO3a responsive promoter (pGL3-p27, pGL3-3xDBE and pGL-6xDBE) assays, 1×10^5 LN229 and T98G cells were reversely transfected in 12-well plates with 0.75 µg of the indicated constructs and 0.25 µg of the control *Renilla* reporter vector. 24 h after transfection cells were either left untreated or treated with 10 µM erlotinib for 24 h. Control and treated cells were harvested 48 h after transfection using a passive-lysis buffer (Promega, Madison, WI, USA) after which luciferase activities were measured. Levels of reporter gene induction were obtained by normalizing *Firefly* luciferase levels to control *Renilla* luciferase levels. The results are presented as the mean ± SD of data from three independent experiments, each of which was conducted in duplicate.

2.7 Gene expression analysis

Total RNA was isolated using Trizol® Reagent (ThermoFisher Scientific, Waltham, MA). One µg RNA was reverse-transcribed into cDNA using a High Capacity RNA-

to-cDNA kit (Applied Biosystems, Los Angeles, CA, USA). Subsequent real-time PCR reactions were performed in 96-well plates in a Light Cycler 480® System (Roche Diagnostics, Basel, Switzerland) using the SYBR® Green detection methodology. FOXO3a mRNA levels were measured using the following primers: *FOXO3a* forward 5'-GGGGAACCTTCACTGGTGCTA, reverse 5'-TGTCCACTTGCTGAGAGCAG. FOXO1 mRNA levels were measured using the following primers: *FOXO1* forward 5'-GCTTCCCACACAGTGTCAAGAC, reverse 5'-CCTGCTGTCAGACAATCTGAAGTAC. p27^{kip1} mRNA levels were measured using the following primers: *CDKN1B* forward 5'-TCCGGCTAACTCTGAGGACA, reverse 5'-GAAGAATCGTCGGTTGCAGG. Cyclin D1 mRNA levels were measured using the following primers: *CCND1* forward 5'-TGTCCTACTACCGCCTCACA, reverse 5'-CAGGGCTTCGATCTGCTC. FOXM1 mRNA levels were measured using the following primers: *FOXM1* forward 5'-ACTTTAAGCACATTGCCAAGC, reverse 5'-CGTGCAGG GAAAGTTGT. *GAPDH* was included as an internal control for normalization and measured using the following primers: *GAPDH* forward 5'-TGCACCACCAACTGCTTAGC, reverse 5'-GGCATGGACTGTGGTCATGAG. Threshold cycle data were analysed using the following formula: normalized gene expression level = $\left(\frac{E_{target}^{C_{P_{target}}(sample)}}}{E_{ref}^{C_{P_{ref}}(sample)}}\right)$ (adapted from [21]) to quantify the levels of gene expression.

2.8 Annexin V/Propidium iodide staining

Phosphatidyl serine externalization in apoptotic cells was determined using an ApoTarget Annexin-V-FITC Apoptosis kit (Life Technologies, Carlsbad, CA, USA), according to the manufacturer's instructions. To this end, 2×10^5 cells were seeded in 6-well plates and treated as indicated. Next, the cells were collected and suspended in 100 μ l Annexin V-binding buffer, after which 5 μ l Annexin-V-FITC and 10 μ l propidium iodide were added and the cells were incubated for 15 min at room temperature in the dark. Finally, flow cytometry was carried out using a FACScan cytometer (Coulter Epics XL-MSL, Beckman Coulter, Fullerton, CA) and analysed using winMDI software.

2.9 Immunofluorescence

Cells grown on coverslips were fixed in 3.7% (v/v) paraformaldehyde for 20 min and permeabilized in 0.1% (v/v) Triton X-100 for 5 min. Cells were blocked in PBS containing 3% bovine serum albumin, after which an antibody directed against FOXO3a (07-702; Millipore, Billerica, MA, USA) was added (1:30 dilution). Specific staining was visualized using a secondary antibody conjugated to Alexa Fluor 488. Coverslips were mounted using mounting medium containing

4',6-diamidino-2-phenylindole (DAPI; Sigma-Aldrich, St. Louis, MO, USA) and analyzed using a Leica TCS SPE confocal microscope (Leica Microsystems, Wetzlar, Germany).

2.10 Subcellular fractionation

Nuclear/cytoplasmic subcellular fractionation was performed using a Nuclear Extract kit (Active Motif, Carlsbad, CA, USA) according to the manufacturer's instructions. Briefly, cells were washed in ice-cold PBS with phosphatase inhibitors, collected by gentle scraping and centrifuged. For fractionation, cell pellets were re-suspended in hypotonic buffer and incubated for 15 min at 4 °C prior to the addition of detergent to lyse the cells. Next, the cytoplasmic fraction was collected by centrifugation (supernatant) and stored at -80 °C. The remaining pellet was subsequently lysed with complete lysis buffer with protease inhibitors, incubated for 30 min at 4 °C and centrifuged to obtain the nuclear fraction (supernatant). Nuclear/cytoplasmic separation was verified through PARP and Tubulin expression analysis using immunoblotting.

2.11 Gel electrophoresis and immunoblotting

For immunoblotting, cells were harvested in a buffer containing 50 mM Tris-HCl pH 7.4, 150 mM NaCl, 1 mM EDTA and 1% (v/v) Triton X-100 plus protease and phosphatase inhibitors. For the detection of nuclear and cytoplasmic FOXO3a levels, cell extracts were collected using a nuclear extract kit (Active Motif, Carlsbad, CA, USA) after which protein content was measured using the Bradford procedure [22]. Cell lysates were electrophoresed using SDS-polyacrylamide gels. After electrophoresis the proteins were transferred to Immobilon-P strips (Millipore, Billerica, MA, USA) for 2 h at 60 V. The resulting blots were preincubated in TBS (20 mM Tris-HCl pH 7.5, 150 mM NaCl), 0.05% Tween 20 and 5% defatted milk powder for 1 h at room temperature and then incubated for 1 h at room temperature in TBS, 0.05% Tween 20, 1% BSA and 0.5% defatted milk powder containing the appropriate antibodies: anti-Akt (sc-1618) and anti-p27^{kip1} (sc-525) from Santa Cruz (Santa Cruz, CA, USA), anti-cyclin D1 (MS-210P, Neomarkers, Fremont, CA), anti- β -tubulin (T0198, Sigma-Aldrich, St. Louis, MO) and anti-p-S473-Akt (#9271), anti-FOXO3a (#9467), anti-p-S253-FOXO3a (#9466), anti-FOXO1 (#2880), anti-PARP (#9542) and anti-p-S6 (#4858) from Cell Signaling Technology (Beverly, MA, USA). After washing in TBS, 0.05% Tween 20, the blots were incubated with a peroxidase-coupled secondary antibody (Dako, Glostrup, Denmark) for 1 h at room temperature. After incubation, the blots were washed twice in TBS, 0.05% Tween 20 and once in TBS. The peroxidase reaction was

visualized using an enhanced chemiluminescence detection system (Millipore, Billerica, MA, USA).

2.12 Statistical analysis

The statistical significance of differences was assessed by Student's *t* test using GraphPad Prism (GraphPad Software Inc. La Jolla, CA). Statistically significant differences are indicated by *** $p < 0.001$, ** $p < 0.01$ and * $p < 0.05$.

3 Results

3.1 EGFR inhibition reduces GBM cell growth and induces FOXO3a dephosphorylation

We have previously shown that EGFR inhibition with erlotinib inhibits glioma cell proliferation by inducing cell cycle arrest in G₁ [10]. In order to better understand the mechanisms underlying sensitivity (and resistance) to EGFR-based therapy in GBM, we set out to investigate molecular mediators responsible for the effects of EGFR inhibition in GBM cells. In agreement with the response to erlotinib in a panel of human GBM cell lines, including cells with mutant EGFR (U87ΔEGFR) or EGFR overexpression (SKMG-3 cells), primary glioma cells derived from patient samples were also found to be sensitive to EGFR inhibition with erlotinib in a dose-dependent manner (Fig. 1a, b). In order to investigate the molecular effects of EGFR inhibition, we used LN229, T98G and U373 cells, which showed high, intermediate and low sensitivities to erlotinib, respectively (Fig. 1a) [10]. Exposure to 10 μM erlotinib induced a time-dependent reduction in p-Akt levels in both LN229 and T98G cells, but not in U373 cells (Fig. 1c). A parallel decrease, observed in all cell lines, was found for p-S6, a target of the mTOR/S6K pathway which acts downstream of PI3K/Akt (Fig. 1c). Interestingly, the reductions in p-Akt and p-S6 were followed, in LN229 and T98G cells, by a time-dependent dephosphorylation of FOXO3a at Ser253, a residue that is phosphorylated by Akt (Fig. 1c).

3.2 EGFR inhibition induces FOXO3a nuclear accumulation and transcriptional activation in glioblastoma cells

Akt-dependent FOXO3a phosphorylation induces its nuclear export and hence sequesters FOXO3a in an inactive state in the cytoplasm [17]. In order to assess whether FOXO3a dephosphorylation induced by EGFR inhibition leads to FOXO3a nuclear accumulation, we analysed the subcellular localization of FOXO3a in control and erlotinib-treated GBM cells. Whereas in untreated cells FOXO3a was mostly

localized in the cytoplasm, EGFR inhibition in LN229, T98G and U373 cells led to its accumulation in the nucleus, especially in the highly-sensitive LN229 cells (Fig. 2a). Importantly, erlotinib treatment also led to FOXO3a nuclear accumulation in primary GBM cells (Fig. 2a). In agreement with these observations, subcellular fractionation experiments also indicated that erlotinib treatment induced a substantial increase in FOXO3a levels in the nuclear fraction (Fig. 2b). Taken together, these results indicate that EGFR inhibition in GBM cells leads to FOXO3a dephosphorylation and its nuclear accumulation.

Since FOXO3a dephosphorylation and nuclear accumulation are required for its transcriptional activity, we next investigated whether erlotinib treatment was able to induce FOXO3a activation in GBM cells. To this end, we first analysed the transcriptional activity of FOXO3a using three different luciferase reporter constructs: one containing the promoter of the FOXO3a transcriptional target p27^{kip1}, and two containing three and six repetitions of the consensus FOXO-binding motif, the DAF-16-binding element (DBE), respectively [23, 24]. We found that erlotinib treatment significantly increased the luciferase activities of the indicated reporters, with the highest values corresponding to a 2–3 fold induction for the 6xDBE reporter (Fig. 2c). We also performed qRT-PCR to measure the mRNA expression levels of the FOXO3a transcriptional targets p27^{kip1} and cyclin D1 (a target of FOXO3a-mediated repression [25]), together with the mRNA levels of FOXO3a and FOXO1, since FOXO transcription factors have been shown to promote their own transcription [26]. In correlation with the data from FOXO3 reporter assays, erlotinib treatment led to an increase in the expression of p27^{kip1} mRNA and a decrease in the expression of cyclin D1 mRNA in both LN229 and T98G cells. U373 cells showed a modest increase in p27^{kip1} mRNA expression levels (Fig. 2d). Interestingly, both FOXO3a and FOXO1 mRNA expression levels were clearly increased upon erlotinib treatment in all cell lines tested, although the effects were more robust in the highly-sensitive LN229 cell line (Fig. 2d). Finally, we confirmed the regulation of FOXO3a target gene expression at the protein level. In agreement with the qRT-PCR data, immunoblot analysis revealed that EGFR inhibition resulted in a strong induction of p27^{kip1} protein expression and a concomitant downregulation of cyclin D1 protein expression (Fig. 2e). Interestingly, FOXO1 expression in response to erlotinib almost mirrored the sensitivity of each cell line, i.e., FOXO1 levels were dramatically increased in LN229 cells, whereas they showed a lower increase in T98G cells. In U373 cells FOXO1 expression remained almost unaltered (Fig. 2e). We also investigated the expression of FOXM1, since this oncogene is also a direct target of FOXO3a-mediated transcriptional repression [27, 28]. Interestingly, in LN229 and T98G cells EGFR inhibition induced a dramatic downregulation of FOXM1, whereas this

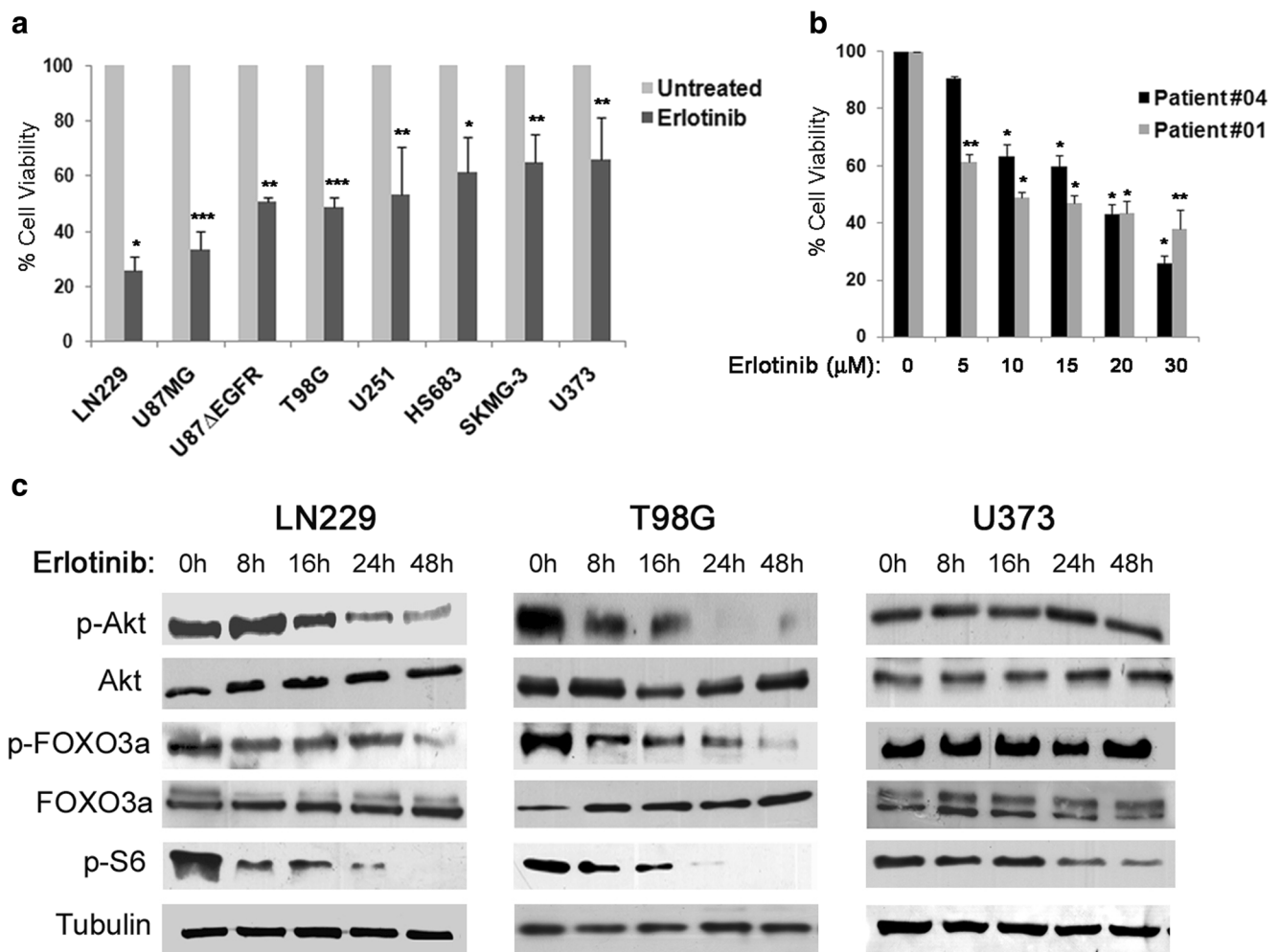


Fig. 1 Erlotinib inhibits glioblastoma cell proliferation and induces FOXO3a dephosphorylation. **a** The indicated glioblastoma cell lines were left untreated (Untreated) or treated with 10 μ M erlotinib (Erlotinib) and cell viability was assessed 48 h after treatment. The mean \pm SD values from three independent experiments, each conducted in duplicate, are shown in the graph, representing the percentage of viable cells relative to untreated conditions. The differences between control and erlotinib treatment are statistically significant (Student's *t* test: * $p < 0.05$, ** $p < 0.01$ and *** $p < 0.001$, respectively). **b** Patient-derived primary glioblastoma cells were treated for 48 h with the indicated concentrations

of erlotinib after which cell viabilities were measured. The mean \pm SD values from three independent experiments, each conducted in duplicate, are shown in the graph, representing the percentage of viable cells relative to untreated conditions. The differences between control and erlotinib treatment are statistically significant (Student's *t* test: * $p < 0.05$, ** $p < 0.01$ and *** $p < 0.001$, respectively). **c** LN229, T98G and U373 cells were treated with 10 μ M erlotinib and harvested at the indicated time points. The expression levels of the indicated proteins were analysed by Western blotting using specific antibodies

effect was more modest in the less sensitive U373 cell line (Fig. 2e). Collectively, these observations indicate that EGFR inhibition in GBM cells leads to activation of FOXO3a and modulation of its transcriptional targets.

3.3 Activation of FOXO3a inhibits glioblastoma cell growth

In order to better understand the contribution of FOXO3a activation in response to EGFR inhibition, we investigated the effects of selective activation of FOXO3a in GBM cells. For this purpose, we treated GBM cells with Psammaplysen A, a compound originally identified as an inhibitor of the

nuclear export of FOXO transcription factors [29] that has been shown to exert in vitro anticancer effects in colon cancer [30], non-Hodgkin lymphoma [31], endometrial cancer [32] and leiomyoma cells [33] through activation of either FOXO3a or FOXO1. We found that treatment of LN229, T98G and U373 cells with 2.5 μ M Psammaplysen A promoted the nuclear accumulation of FOXO3a (Fig. 3a). A time-course treatment with Psammaplysen A confirmed FOXO3a activation as indicated by its dephosphorylation at S253 (Fig. 3b). Interestingly, Psammaplysen A treatment also induced an increase in total FOXO3a expression levels, and modulation of FOXO3a target genes p27^{kip1}, cyclin D1, FOXO1 and FOXM1 (Fig. 3b). Of note, p-Akt levels were

not altered by Psammaplysene A treatment, confirming previous reports showing that FOXO3a activation induced by this compound does not alter the activity of its upstream kinase Akt [29]. Importantly, in agreement with its ability to promote FOXO3a nuclear accumulation and activation, we found that Psammaplysene A exerted significant *in vitro* antitumoral effects in human GBM cells (Fig. 3c).

In order to further test the effects of FOXO3a activation in GBM, we transfected LN229, T98G and U373 cells with a triple-alanine FOXO3a mutant that cannot be phosphorylated by Akt (FOXO3a-A3) and is, hence, considered to be an active mutant. In agreement with the data obtained using Psammaplysene A, we found that transfection of a FOXO3a-A3 plasmid significantly reduced cell viability compared to that of control transfectants (Fig. 3d). Finally, we also tested the efficacy of trifluoperazine in GBM cell lines and patient-derived cells, since this agent was also identified as a nuclear export inhibitor of FOXO [29] and has been shown to promote FOXO1 activation in human lung adenocarcinoma cells [34]. In agreement with these reports and our previous observations, treatment with trifluoperazine dramatically reduced the viability of both GBM cell lines and primary patient-derived cells, with IC_{50} values in the low micromolar range (Fig. 3e–g), in correlation with its ability to promote FOXO1 and FOXO3a nuclear localization and dephosphorylation in GBM cells (data not shown).

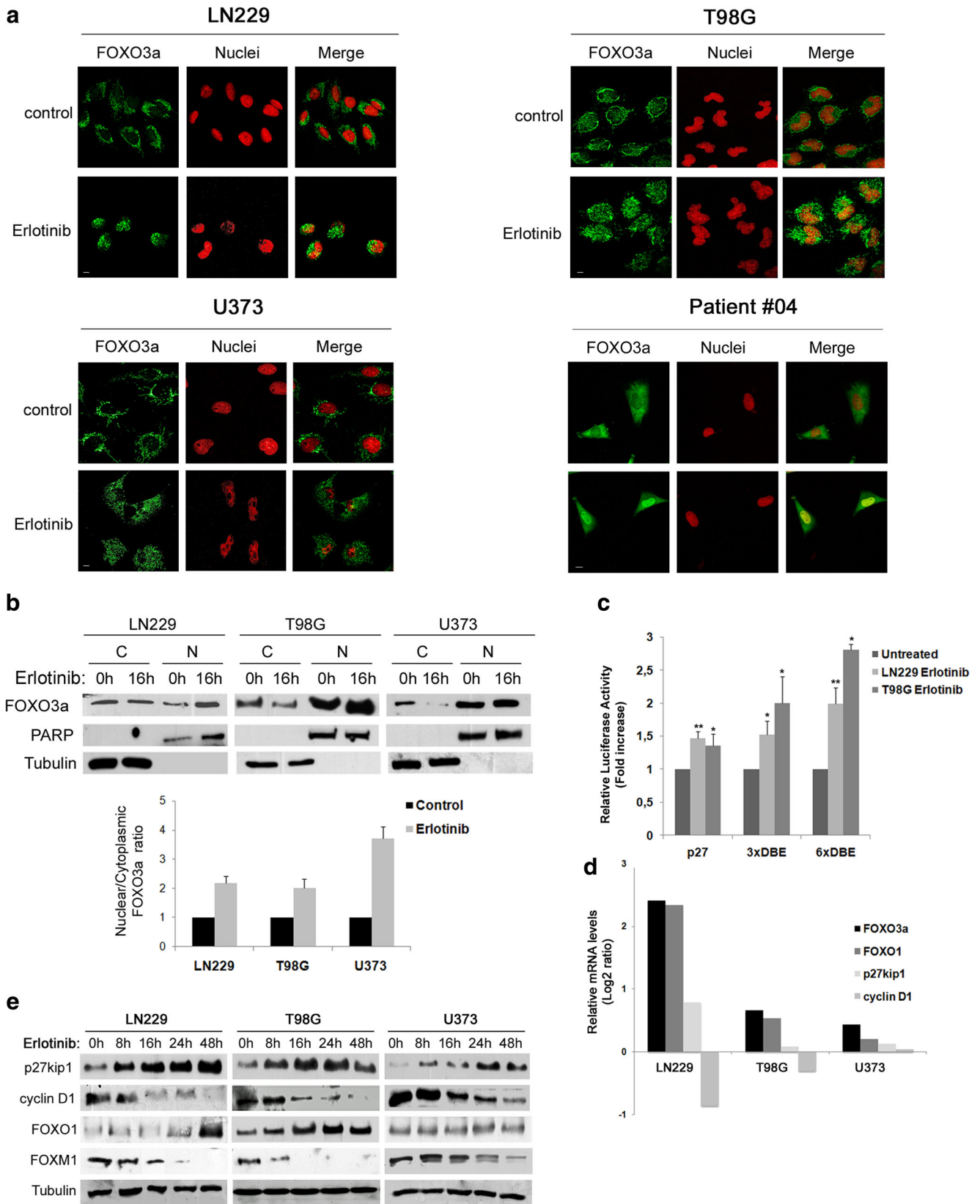
3.4 FOXO3a activation cooperates synergistically with EGFR inhibition in glioblastoma cells

In order to test the therapeutic potential of FOXO3a modulation in combination with EGFR inhibition, we first assessed the effects of erlotinib in control versus FOXO3a-A3 transfected cells. Whereas erlotinib treatment or FOXO3a-A3 transfection alone clearly reduced GBM cell growth, the combination of erlotinib treatment and FOXO3a-A3 expression totally suppressed GBM cell growth and even resulted in a net decrease in cell number, suggestive of cell death (Fig. 4a). We next used trifluoperazine to test whether pharmacological activation of FOXO3a could similarly cooperate with erlotinib to reduce GBM cell growth. We chose trifluoperazine instead of Psammaplysene A because it is a FDA-approved drug with a well-established clinical use, and because it has been recently reported to sensitize lung adenocarcinoma cells to erlotinib [34]. Treatment of GBM cell lines and primary patient-derived cells with erlotinib alone or in combination with a fixed dose of trifluoperazine (5 μ M, 7.5 μ M or 10 μ M) indicated that trifluoperazine cooperated in a dose-dependent manner with EGFR inhibition in reducing GBM cell viability (Fig. 4b). Accordingly, we found that addition of 10 μ M trifluoperazine resulted in a clear improvement in the IC_{50} of erlotinib, with an average 6-fold reduction, both

in cell lines and primary cells (Fig. 4c). Noteworthy, we found that addition of trifluoperazine dramatically improved the effects of erlotinib on the low sensitive U373 cell line (Fig. 4b), as indicated by the 15-fold decrease observed in IC_{50} value of erlotinib in the presence of 10 μ M trifluoperazine (Fig. 4c). Since these results support a positive pharmacological cooperation between trifluoperazine and EGFR inhibition, in line with data reported in lung adenocarcinoma [34], we next performed isobolographic analyses upon fixed dose-ratio combination treatments with erlotinib and trifluoperazine. To this end, LN229, T98G, U373 and primary patient-derived cells were treated with a number of erlotinib/trifluoperazine combinations (ranging from 1:1 to 1:10) after which the resulting IC_{50} values were plotted on isobolograms indicating the isoeffective line of pure additivity (Fig. 4d). Importantly, virtually all tested combinations resulted in a supra-additive, synergistic interaction between erlotinib and trifluoperazine (Fig. 4d), as indicated also by the determined values of the respective combination indexes (CI, Table 1). Taken together, these results indicate that the FOXO modulator trifluoperazine cooperates synergistically with the EGFR inhibitor erlotinib in reducing GBM cell growth.

3.5 FOXO3a activation with trifluoperazine enhances the cellular and molecular effects of EGFR inhibition

In order to better understand the molecular basis of the synergistic cooperation between EGFR inhibition and FOXO3a activation, we next assessed the effects of the combined treatment with erlotinib and trifluoperazine in patient-derived primary glioma cells. To this end, we first measured the induction of apoptosis through double Annexin V/Propidium Iodide staining in primary glioblastoma cells derived from 2 patients upon treatment with either 10 μ M erlotinib, 10 μ M trifluoperazine or their combination. Interestingly, we found that whereas treatment with erlotinib or trifluoperazine alone did not induce any significant changes in the basal levels of apoptosis detected in untreated cells, the combination of erlotinib and trifluoperazine was able to promote a significant 2-fold increase in the Annexin V-positive population (Fig. 5a). In correlation with this, the combination of erlotinib and trifluoperazine, in contrast to either treatment alone, was also able to significantly induce activation of the effector caspases 3/7 in patient-derived cells (Fig. 5b). Importantly, the combination of erlotinib and trifluoperazine treatment induced a clear dephosphorylation of FOXO3a at Ser253, in contrast to a more modest effect elicited by either treatment alone (Fig. 5c). In agreement with its dephosphorylation and functional activation, we found that total FOXO3a levels were increased after the combination treatment, and that the expression of the FOXO3a targets FOXM1, cyclin D1 and p27^{kip1} was modulated accordingly



in response to the combination of EGFR inhibition and trifluoperazine treatment (Fig. 5c). Taken together, these data

indicate that FOXO3a activation with trifluoperazine enhances the response to EGFR inhibition in GBM cells.

Fig. 2 EGFR inhibition induces FOXO3a nuclear accumulation and its transcriptional activation. **a** The indicated glioblastoma cells were grown on coverslips and were left untreated (control) or were treated for 24 h with 10 μ M erlotinib (erlotinib), fixed and stained with anti-FOXO3a antibodies (FOXO3a) and DAPI (Nuclei). Bar: 5 μ m. **b** The indicated glioblastoma cells were left untreated (control) or were treated for 16 h with 10 μ M erlotinib (erlotinib), harvested and subjected to subcellular fractionation as indicated in Materials and methods. The expression levels of the indicated proteins in cytoplasmic (C) and nuclear (N) cellular extracts were analysed by Western blotting using specific antibodies. The graph represents the mean \pm SD values of quantified nuclear/cytoplasmic FOXO3a ratio, relative to untreated cells. **c** Representation of the mean \pm SD values of luciferase activity from three different FOXO3a reporter constructs (p27, 3xDBE and 6xDBE) in control and erlotinib-treated LN229 and T98G cells, measured as indicated in Materials and methods, from three independent experiments each conducted in duplicate. **d** The levels of the indicated FOXO3a transcriptional targets were measured by qRT-PCR in control and erlotinib-treated (10 μ M, 16 h) LN229, T98G and U373 cells. The graph represents the mean \pm SD Log₂ ratio values of normalized mRNA levels in erlotinib-treated LN229, T98G and U373 cells (control value for each cell line is 0). **e** LN229, T98G and U373 cells were treated with 10 μ M erlotinib and harvested at the indicated time points. The expression levels of the indicated proteins were analysed by Western blotting using specific antibodies

3.6 FOXO3a is a crucial mediator of the effects of EGFR inhibition in glioblastoma cells

We finally investigated the functional contribution of FOXO3a to the effects of EGFR inhibition by silencing FOXO3a in GBM cells. For this purpose, cells were transfected with either scramble (shCONT) or FOXO3a-specific (shFOXO3a) shRNA constructs in order to generate control and FOXO3a-depleted LN229, T98G and U373 cells, respectively (Fig. 6a). We next analysed the cellular effects of EGFR inhibition by treating both control and FOXO3a-depleted cells for 48 h with increasing concentrations of erlotinib. As expected, erlotinib treatment resulted in a clear dose-dependent reduction in cell viability in shCONT-transfected cells (Fig. 6b). This response was, however, strongly diminished in shFOXO3a-transfected cells, which only showed a marginal effect upon erlotinib treatment (Fig. 6b). In conformity with these results, we found that the IC₅₀ values of erlotinib in FOXO3a-depleted cells were clearly higher than those obtained in control cells (Fig. 6c). We also assessed the impact of FOXO3a silencing on the highly effective combination treatment with erlotinib and trifluoperazine. In agreement with our previous results in patient-derived primary cells (Fig. 5b), we found that treatment of shCONT-transfected LN229, T98G and U373 cells with the combination of 10 μ M erlotinib and 10 μ M trifluoperazine induced a clear upregulation of caspase 3/7 activity, whereas either treatment alone had negligible effects (Fig. 6d). Remarkably, FOXO3a silencing in LN229, T98G and U373 cells led to a complete suppression of caspase 3/7 activation in response to the combination treatment with erlotinib plus trifluoperazine (Fig. 6d). Finally, we investigated

the molecular responses elicited by treatment with erlotinib, trifluoperazine or their combination in control and FOXO3a-depleted LN229 cells. We found that in shCONT-transfected LN229 cells, both erlotinib and trifluoperazine treatments alone induced increases in FOXO3a and p27^{kip1} levels and a decrease in cyclin D1 levels, and that these effects were more robust when the cells were treated with the combination of erlotinib and trifluoperazine (Fig. 6e). In contrast, treatment of shFOXO3a-transfected LN229 cells with erlotinib, trifluoperazine or their combination failed to produce such effects on p27^{kip1} and cyclin D1 expression levels (Fig. 6e).

4 Discussion

Here, we have investigated the functional role of the tumor suppressor FOXO3a in the response to EGFR inhibition in malignant GBM cells. Emerging evidence has highlighted a crucial role of the PI3K/Akt signaling flux as a key determinant in the response to EGFR inhibitors in glioma [5], and a number of studies has employed various strategies to target the PI3K/Akt/mTOR pathway in GBM cells with the aim to increase their sensitivity to EGFR inhibitors [13–15]. However, the specific role of the transcription factor FOXO3a, a major Akt target that has been reported to be crucially involved in the cellular response to a growing number of anticancer agents [19], has not been explored yet in this context. In agreement with our previously reported data [10], we found that both established GBM cell lines and patient-derived primary cells responded in a dose-dependent manner to the EGFR inhibitor erlotinib, in correlation with the observed inhibition of PI3K/Akt/mTOR signaling, as indicated by the inhibition of p-Akt and p-S6 levels. Interestingly, we found that a reduction in FOXO3a phosphorylation at S253, indicative of its functional activation, also occurred in response to erlotinib treatment. Accordingly, EGFR inhibition promoted the nuclear translocation of FOXO3a and the modulation of established FOXO3a transcriptional targets, including FOXM1, p27^{kip1} and cyclin D1, together with increases in FOXO3a transcriptional activity in gene reporter assays. The observation that EGFR inhibition leads to FOXM1 downregulation is relevant, since this member of the Forkhead family of transcription factors is emerging as an oncogene in GBM. FOXM1, a well-established regulator of cell cycle progression [35], has been shown to be overexpressed in GBMs [36] and to promote invasion [37], angiogenesis [38], stemness [39–41] and resistance to radio- [39] and chemotherapy [42]. Despite its well-established role in gliomagenesis, partially through the regulation of Wnt/ β -catenin signaling [43], the precise regulation of FOXM1 expression and activity in GBM cells is less well defined. Here, we present the first evidence linking the response to EGFR inhibition in GBM cells to FOXO3a-mediated FOXM1 downregulation. Interestingly, stimulation of GBM cells with EGF has been reported to promote COX-2

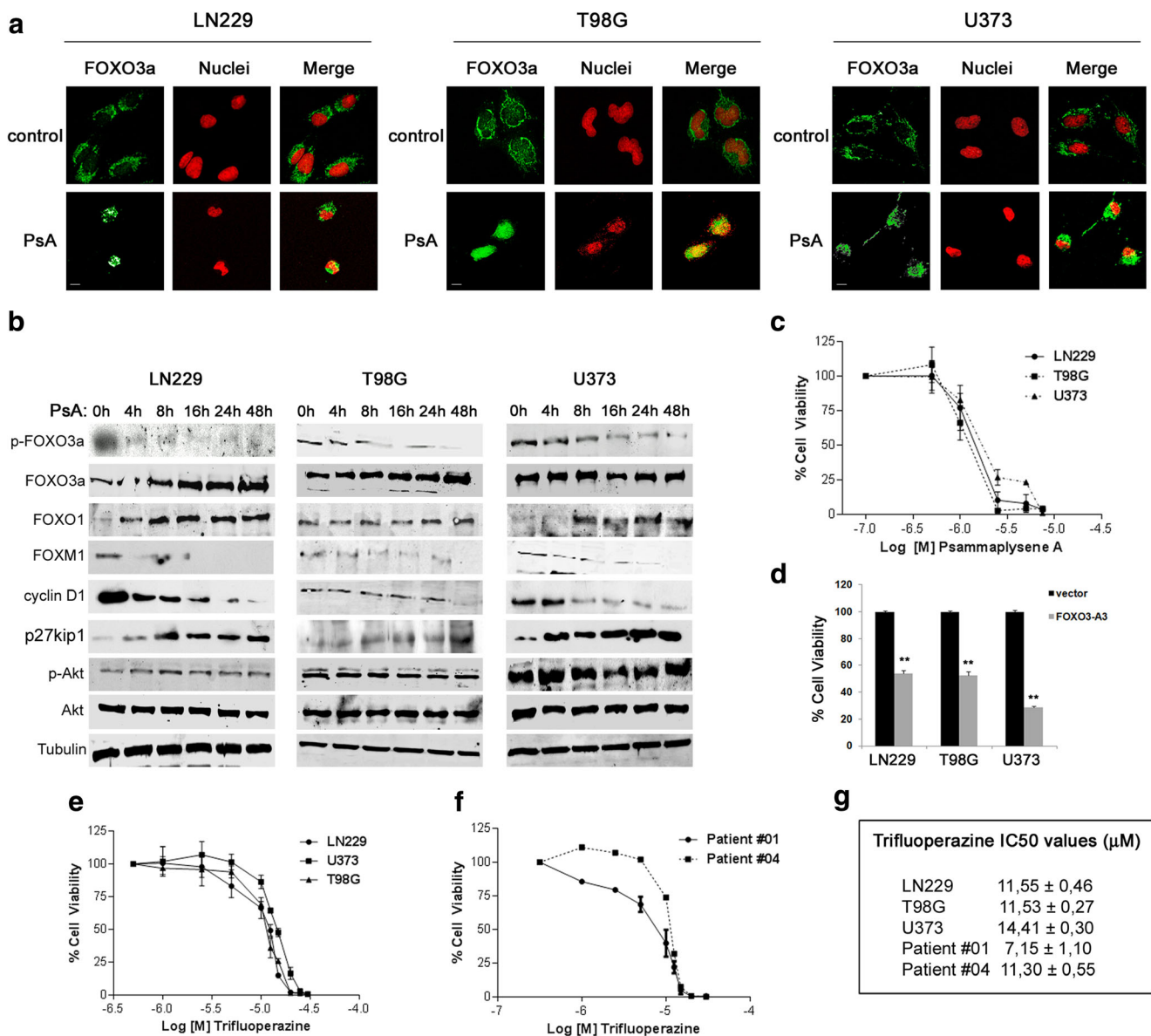


Fig. 3 FOXO3a re-activation inhibits glioblastoma cell growth. **a** LN229, T98G and U373 cells were grown on coverslips and were left untreated (control) or were treated for 24 h with 2.5 μM Psammaplysene A (PsA), fixed and stained with anti-FOXO3a antibodies (FOXO3a) and DAPI (Nuclei). Bar: 5 μm. **b** LN229, T98G and U373 cells were treated with 2.5 μM Psammaplysene A (PsA) and harvested at the indicated time points. The expression levels of the indicated proteins were analysed by Western blotting using specific antibodies. **c** LN229, T98G and U373 cells were treated with increasing concentrations of Psammaplysene A after which cell viabilities were measured. The mean ± SD values from three independent experiments, each conducted in duplicate, are shown in the graph, representing the percentage of viable cells relative to untreated conditions for each tested concentration (expressed as Log [M]). **d** LN229, T98G and U373 cells were transfected with an activated FOXO3a expression plasmid (FOXO3a-A3) or the corresponding

empty vector (vector) after which cell viabilities were measured 48 h upon transfection. The mean ± SD values from three independent experiments, each conducted in duplicate, are shown in the graph, representing the percentage of viable cells for each cell line relative to empty vector-transfected cells. The differences between empty vector and FOXO3a-A3 transfections are statistically significant (Student's *t* test: ***p* < 0.01). **e** and **f** LN229, T98G and U373 cells (**e**) or patient-derived primary glioma cells (**f**) were treated with increasing concentrations of trifluoperazine and cell viability was measured. The mean ± SD values from three independent experiments, each conducted in duplicate, are shown in the graph, representing the percentage of viable cells relative to untreated conditions for each tested concentration (expressed as Log [M]). **g** Mean ± SD IC₅₀ values for trifluoperazine in the indicated glioblastoma cell lines and patient-derived cells, obtained from the viability data shown in (**e**) and (**f**) through non-linear regression analysis

expression through FOXM1 [44], thus indicating that FOXM1 may be regulated downstream of EGFR in GBM. In agreement with our data, FOXO3a dephosphorylation and its nuclear translocation have similarly been shown to mediate the effects of the

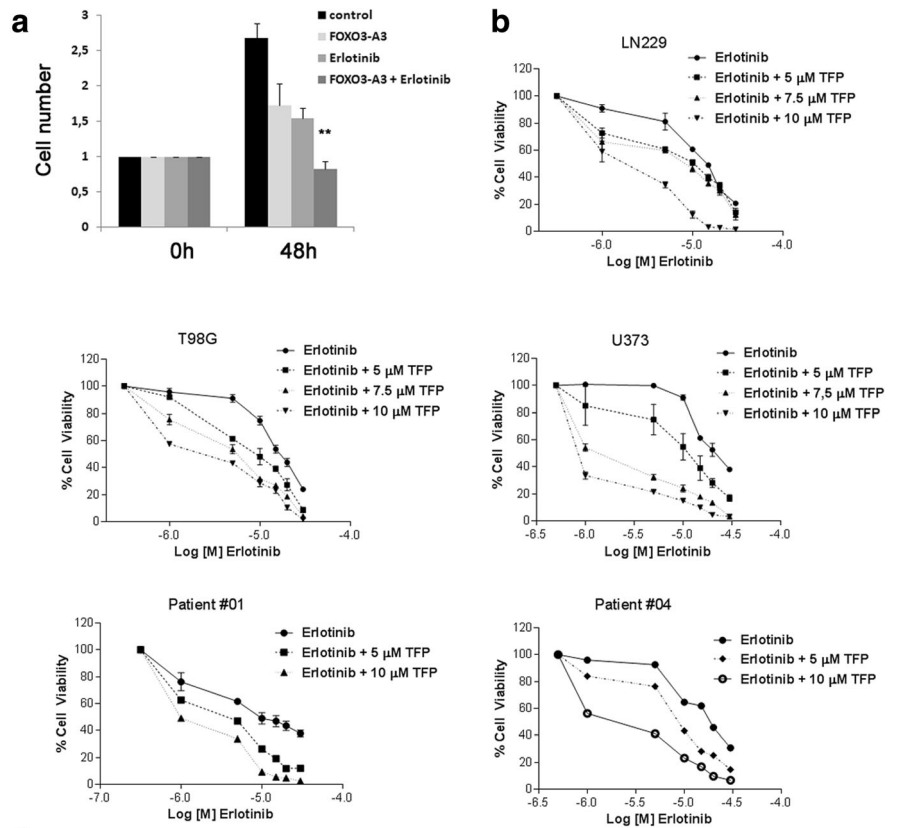
EGFR inhibitor gefitinib in breast cancer cells [45]. Furthermore, in breast cancer cells FOXO3a has been reported to mediate direct transcriptional repression of FOXM1 in response to EGFR inhibition [27]. These results are in agreement

Fig. 4 Activation of FOXO3a cooperates synergistically with EGFR inhibition in glioblastoma cells.

a LN229 cells were transfected with an empty vector (control) or an activated FOXO3a construct (FOXO3a-A3) and left either untreated or treated for 48 h with 10 μ M erlotinib (Erlotinib), (FOXO3a-A3 + Erlotinib) after which cell viability was measured. The mean \pm SD values from three independent experiments, each conducted in duplicate, are shown in the graph, representing the fold increases in cell number relative to time zero. **b** LN229, T98G, U373 and patient-derived primary glioblastoma cells were treated with increasing concentrations of erlotinib alone or in the presence of a fixed dose of trifluoperazine (TFP) after which cell viability was measured. The mean \pm SD values from three independent experiments, each conducted in duplicate, are shown in the graph, representing the percentage of viable cells relative to untreated conditions for each tested concentration of erlotinib (expressed as Log [M]).

c Mean \pm SD IC_{50} values for erlotinib alone or in combination with a fixed dose of trifluoperazine (TFP) in the indicated GBM cell lines and patient-derived cells, obtained from the viability data shown in (b) through non-linear regression analysis.

d LN229, T98G, U373 and patient-derived primary glioblastoma cells were treated with fixed dose ratio combinations (a = 1:1, b = 1:2, c = 1:3, d = 3:1, e = 2:1, f = 1:4, g = 1:5, h = 1:10) of erlotinib and trifluoperazine. Isobolographic analyses were performed as described in the Materials and methods section. Data shown in the isobolograms are means \pm SD from three independent determinations performed in duplicate. Each isobologram shows the IC_{50} value of trifluoperazine on the Y-axis and the IC_{50} of erlotinib on the X-axis, connected by the iso-effective line of theoretical additivity



| | <u>IC50 values (μM)</u> | | | | |
|-----------------------------|--|------------------|------------------|------------------|------------------|
| | LN229 | T98G | U373 | Patient #01 | Patient #04 |
| Erlotinib | 13.06 \pm 0.83 | 16.90 \pm 0.60 | 21.76 \pm 1.60 | 11.42 \pm 1.80 | 15.12 \pm 0.66 |
| Erlotinib + 5 μ M TFP | 7.86 \pm 1.50 | 8.48 \pm 0.89 | 9.92 \pm 1.80 | 3.02 \pm 0.61 | 8.80 \pm 1.80 |
| Erlotinib + 7.5 μ M TFP | 6.31 \pm 1.48 | 4.80 \pm 0.71 | 2.43 \pm 0.50 | n.d. | n.d. |
| Erlotinib + 10 μ M TFP | 1.95 \pm 0.40 | 2.80 \pm 0.52 | 1.33 \pm 0.32 | 1.47 \pm 0.30 | 2.73 \pm 0.81 |

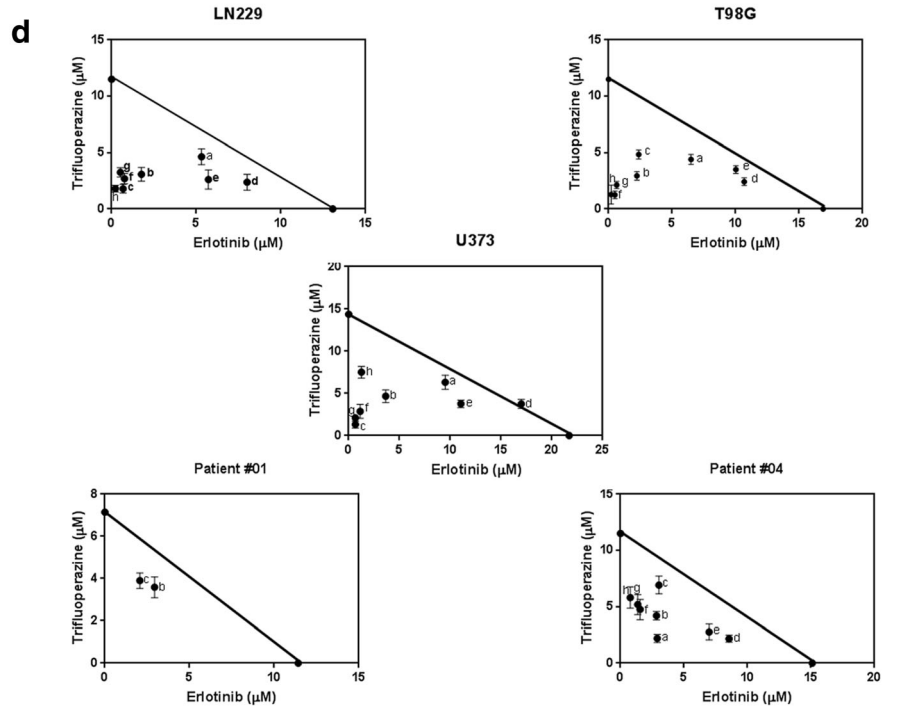


Table 1 Combination Indexes of erlotinib and trifluoperazine combinations

| Combination | Erlotinib:TFP proportion | LN229 | T98G | U373 | Patient #01 | Patient #04 |
|-------------|--------------------------|-------|------|------|-------------|-------------|
| <i>a</i> | (1:1) | 0.80 | 0.76 | 0.86 | n.d. | 0.38 |
| <i>b</i> | (1:2) | 0.40 | 0.38 | 0.48 | 0.75 | 0.54 |
| <i>c</i> | (1:3) | 0.20 | 0.56 | 0.12 | 0.72 | 0.80 |
| <i>d</i> | (3:1) | 0.81 | 0.84 | 1.04 | n.d. | 0.74 |
| <i>e</i> | (2:1) | 0.65 | 0.89 | 0.76 | n.d. | 0.70 |
| <i>f</i> | (1:4) | 0.29 | 0.14 | 0.25 | n.d. | 0.51 |
| <i>g</i> | (1:5) | 0.29 | 0.22 | 0.17 | n.d. | 0.54 |
| <i>h</i> | (1:10) | 0.17 | 0.12 | 0.58 | n.d. | 0.55 |

The table shows all tested erlotinib and trifluoperazine (TFP) combinations in each cell line or patient-derived cell culture, indicating the proportion of each drug in all combinations and the resulting Combination Indexes (CI). Combinations with CI > 1 are considered as antagonistic, those with CI = 1 as additive, and those with CI < 1 as synergistic

with several other studies reporting that FOXO3a activation mediates the cellular responses to established chemotherapeutic agents including imatinib, paclitaxel and cisplatin in chronic myeloid leukemia (CML), breast cancer and colorectal cancer, respectively [30, 46, 47]. In some cases, FOXM1

downregulation downstream of FOXO3a has been shown to participate in these responses, fueling the concept that the FOXO3a-FOXM1 axis may serve as a promising therapeutic target [48]. In this vein, TIC10, an orally-available activator of TRAIL has recently been shown to induce antitumor effects in

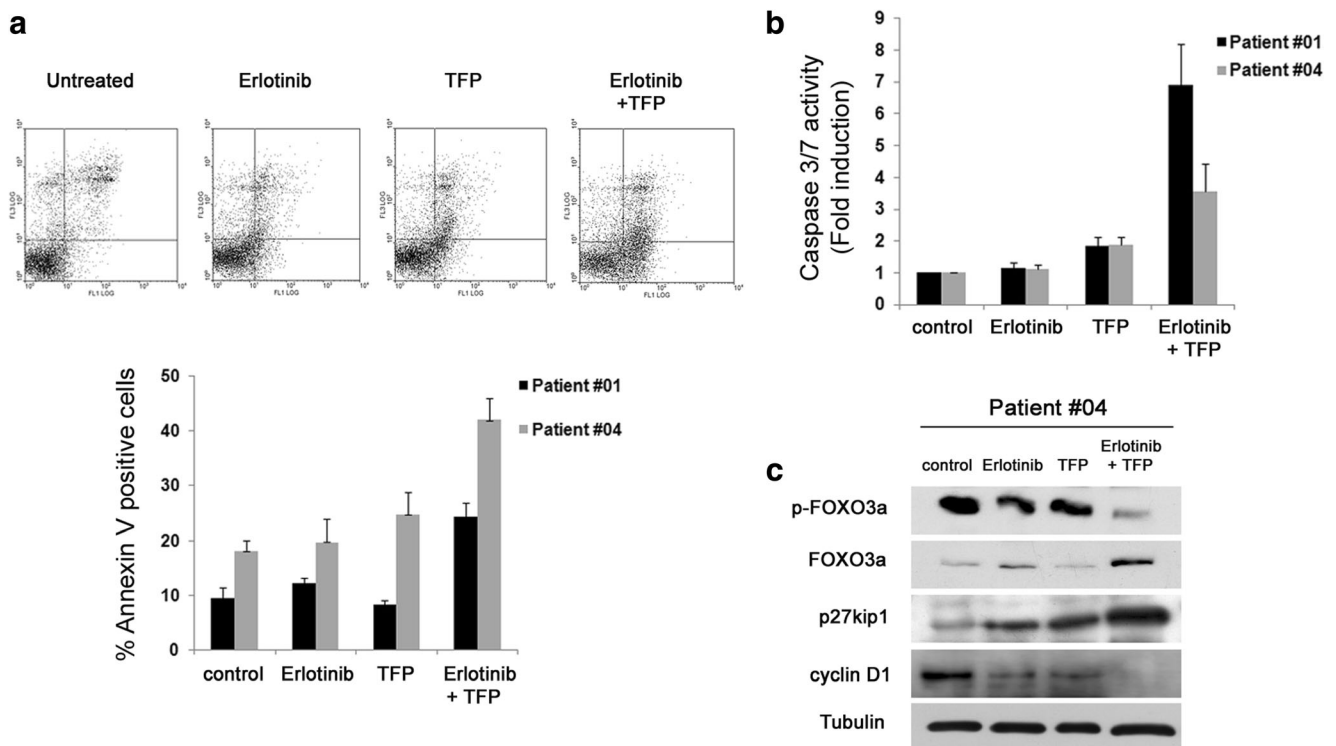


Fig. 5 FOXO3a activation with trifluoperazine enhances the cellular and molecular effects of EGFR inhibition. **a** Patient-derived primary glioblastoma cells were left untreated (Untreated) or treated with 10 μ M erlotinib (Erlotinib), 10 μ M trifluoperazine (TFP) or the combination of both (Erlotinib + TFP). Cells were harvested at 48 h, stained with Annexin V-FITC/Propidium Iodide and analysed by flow cytometry as described in Materials and methods. The dot plot (top) is a representative example of Patient #04-derived cells, showing Annexin V-FITC staining (X-axis) and Propidium iodide staining (Y-axis). The graph (bottom) represents the mean \pm SD percentage values of the Annexin V-positive

cell population in the indicated patient-derived cells. **b** Patient-derived primary glioblastoma cells were treated as in (a) after which Caspase 3/7 activity was measured as indicated in Materials and methods. The data show the mean \pm SD values from three independent experiments, each conducted in triplicate, representing the fold induction in caspase activity relative to untreated cells. **c** Patient-derived primary glioblastoma cells were treated as in (a) and (b) and harvested at 24 h. The expression levels of the indicated proteins were analysed by Western blotting using specific antibodies

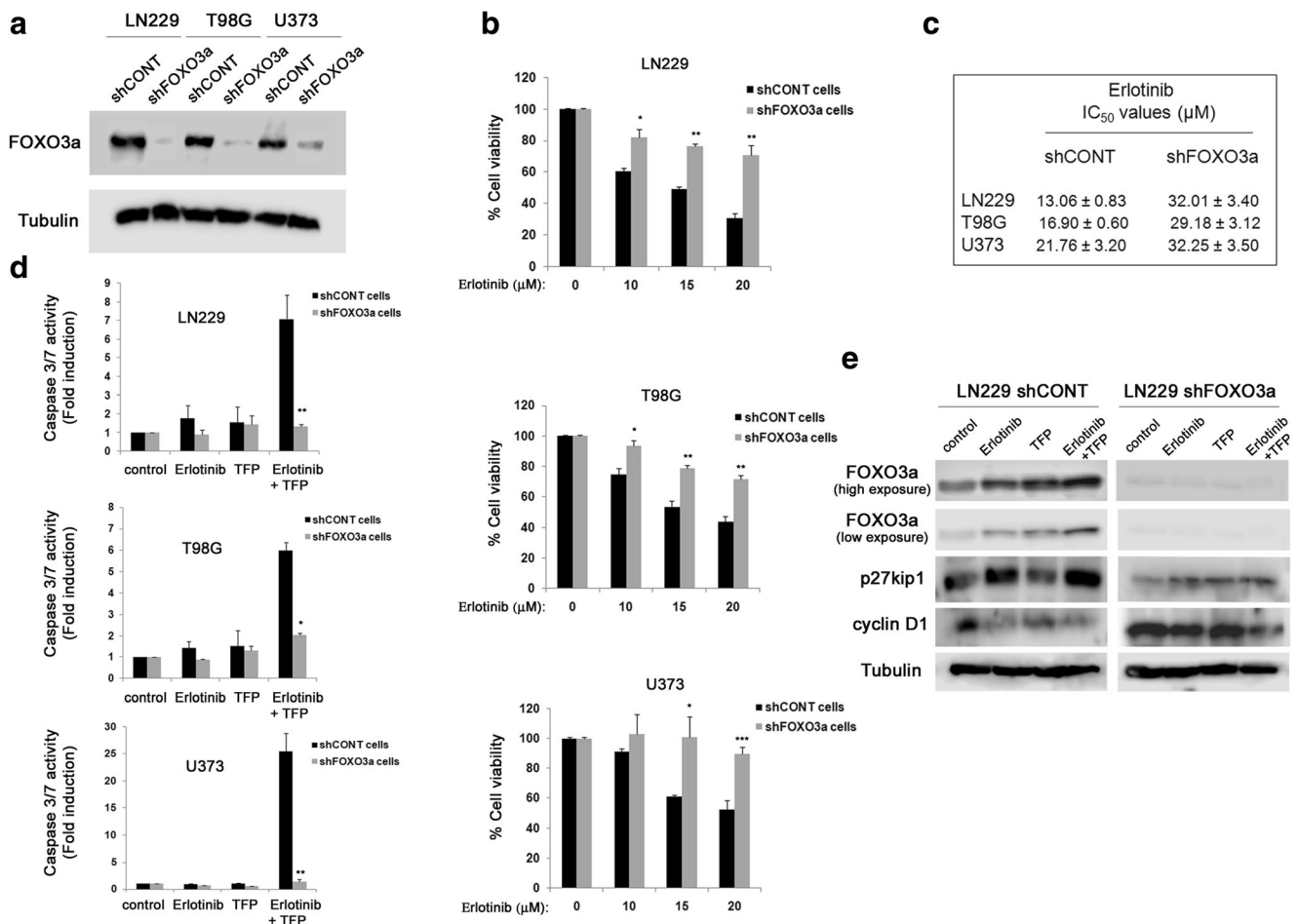


Fig. 6 FOXO3a is a crucial mediator of the effects of EGFR inhibition in glioblastoma cells. **a** LN229, T98G and U373 cells were transfected with a control shRNA (shCONT) or a shRNA targeting human FOXO3a (shFOXO3a) after which stable transfectants were generated as indicated in Materials and methods. Control and FOXO3a-depleted cells were harvested and the expression levels of FOXO3a and β -Tubulin (loading control) were analysed by Western blotting using specific antibodies. **b** Control (shCONT) and FOXO3a-depleted (shFOXO3a) LN229, T98G and U373 cells were treated for 48 h with the indicated concentrations of erlotinib and cell viability was measured. The mean \pm SD values from three independent experiments, each conducted in duplicate, are shown in the graph, representing the percentage of viable cells relative to untreated conditions. The differences between shCONT and shFOXO3a cells are statistically significant (Student's *t* test: * p < 0.05, ** p < 0.01 and *** p < 0.001, respectively). **c** Control (shCONT) and FOXO3a-depleted (shFOXO3a) LN229, T98G and U373 cells were treated for 48 h with increasing

concentrations of erlotinib after which cell viability was measured. Data were processed through non-linear regression analysis to obtain the indicated mean \pm SD IC₅₀ values for erlotinib in each of the transfected cell lines. **d** Control (shCONT) and FOXO3a-depleted (shFOXO3a) LN229, T98G and U373 cells were left untreated (control) or treated with 10 μ M erlotinib alone (Erlotinib), 10 μ M trifluoperazine alone (TFP) or the combination of both (Erlotinib + TFP) and Caspase 3/7 activity was measured at 48 h. The data show the mean \pm SD values from three independent experiments, each conducted in triplicate, representing the fold induction in caspase activity relative to untreated cells. The differences between shCONT and shFOXO3a cells are statistically significant (Student's *t* test: * p < 0.05 and ** p < 0.01, respectively). **e** Control (shCONT) and FOXO3a-depleted (shFOXO3a) LN229 cells were treated as in **(d)** and harvested at 24 h. The expression levels of the indicated proteins were analysed by western blotting using specific antibodies

GBM cells through nuclear translocation of FOXO3a [49], further suggesting that pharmacological activation of FOXO3a may constitute an attractive therapeutic strategy.

Our results clearly support other reports indicating that FOXO3a exerts a tumor suppressor role in GBM, since low FOXO3a levels have been linked to a poor prognosis [18], and FOXO3a activation has been shown to induce differentiation of glioma stem cells (GSCs) and to reduce tumorigenicity [50]. In contrast, however, a recent report

has suggested that FOXO3a overexpression may be linked to GBM progression and a poor prognosis [51], possibly reflecting methodological differences such as the selection of antibodies used for immunohistochemistry.

Interestingly, activation of FOXO3a in GBM cells using Psammalyse A, a FOXO nuclear export inhibitor [30, 31, 52], clearly decreased cell viabilities and promoted molecular responses similar to those of erlotinib, i.e., dephosphorylation and nuclear translocation of FOXO3a followed by modulation

of its transcriptional targets FOXO1, FOXM1, cyclin D1 and p27^{kip1}. It should be noted, however, that direct activation of FOXO1 may also contribute to the observed effects of Psammaplysene A in GBM cells, since this compound is a general FOXO nuclear export inhibitor. Furthermore, treatment with trifluoperazine, another compound that has also been reported to promote FOXO nuclear export inhibition [29], and transfection of a triple-alanine active FOXO3a mutant similarly led to decreased GBM cell viability. The efficacy of trifluoperazine in GBM cells is noteworthy, since this FDA-approved dopamine receptor antagonist traverses the blood-brain barrier and is a clinically-established antipsychotic agent. However, it should be noted that the plasma levels of trifluoperazine in psychotic patients are in the nanomolar range [53], indicating that this drug is not the best candidate for the treatment of GBM patients. In contrast, related phenothiazine drugs such as thioridazine, with plasma levels in the micromolar range [54], may be better suited as co-adjuvants for the treatment of GBM.

We found that trifluoperazine was similarly effective against GBM cell lines and primary GBM cell cultures, with an IC₅₀ in the low micromolar range. These results are in agreement with others describing in vitro anticancer activities of related phenothiazine compounds in GBM cells [55–57] (reviewed in [58]). These results suggest that dopamine receptor signaling in GBM cells may modulate FOXO3a activity, since the primary cellular targets of phenothiazines are dopamine receptors. It should be noted, however, that trifluoperazine is also a well-established Calmodulin (CaM) inhibitor [59]. In this vein, CaM inhibition has been shown to induce FOXO1 and FOXO3a nuclear localization in 786-O renal cell adenocarcinoma [29] and U2OS osteosarcoma [60] cells, respectively. This suggests that a CaM-dependent mechanism may be responsible for FOXO nuclear relocation induced by trifluoperazine, although this hypothesis still needs to be tested in GBM cells, together with the precise molecular mechanism linking CaM to FOXO3a nuclear localization.

Interestingly, addition of trifluoperazine was able to increase the sensitivity of GBM cell lines and primary cells to erlotinib, in correlation with its ability to restore the sensitivity to erlotinib through FOXO1 modulation in erlotinib-resistant lung adenocarcinoma cells [34]. Moreover, our isobolographic analyses after fixed-dose ratio combinations confirmed the synergistic cooperation between erlotinib and trifluoperazine in GBM cell lines and primary cells, similarly to that reported in lung adenocarcinoma [34]. Importantly, our results from GBM patient-derived primary cells suggest that the erlotinib/trifluoperazine combination, in contrast to either treatment alone, is able to promote apoptosis rather than cell cycle arrest. This cytostatic to cytotoxic switch likely reflects enhanced activation of FOXO3a, as indicated by the dramatic dephosphorylation of FOXO3a and the robust modulation of its transcriptional targets cyclin D1 and p27^{kip1} observed upon

treatment with the erlotinib/trifluoperazine combination. Our results are in agreement with a recent report indicating that inhibition of dopamine receptor 2 with the antipsychotic haloperidol exerts synergistic antitumor activity with EGFR inhibitors in glioblastoma models [61].

Importantly, we found that FOXO3a silencing strongly inhibited the cellular effects of erlotinib, clearly indicating that FOXO3a is an essential mediator of the cellular response to EGFR inhibition, which is in agreement with the crucial role of FOXO3a activation in mediating the response to a growing number of antitumor agents [19]. Remarkably, the induction of apoptosis observed upon treatment of GBM cells with the erlotinib/trifluoperazine combination was completely suppressed upon FOXO3a depletion, in correlation with the impaired ability of FOXO3a-depleted cells to modulate the expression of FOXO3a transcriptional targets. These results suggest that FOXO3a nuclear relocation is also responsible for the antitumor activity of trifluoperazine in GBM cells.

Altogether, the major conclusions of our work are that: 1) FOXO3a activation is essential for the response of GBM cells to EGFR inhibition, and 2) FOXO3a may serve as a promising actionable therapeutic target in GBM.

These observations are important for a number of reasons. Firstly, because they highlight for the first time a central role of the PI3K/Akt downstream target FOXO3a in the anti-EGFR therapy response, which is a major therapeutic challenge in GBM. Secondly, because they may have therapeutic implications, since FDA-approved antipsychotic phenothiazines may sensitize otherwise resistant cells to EGFR inhibitors, thereby improving their clinical efficacy, or may cooperate with other anti-GBM agents, including the standard chemotherapeutic agent temozolomide (TMZ). Our data pave the way for investigating the potential of FOXO modulators, such as phenothiazines, as co-adjuvants for the treatment of GBM.

Acknowledgements We are grateful to Joan Seoane (Institut de Recerca Hospital Vall d'Hebron, Barcelona), Hans Skovgaard (Rigshospitalet, Oslo) and Isabel Martínez-Lacaci (Hospital Universitario Virgen de la Arrixaca, Murcia) for the gift of human glioma cell lines, to Jon Clardy (Harvard University) for Psammaplysene A and to Eric W-F Lam (Imperial College London) and Wolfgang Link (CNIO, Madrid) for expression plasmids. We are also grateful to Roche for providing erlotinib hydrochloride. The Cancer Cell Biology Laboratory is supported by a Consolider Ingenio grant (CSD2010-00065, Ministerio de Economía y Competitividad, Spain, to G.R., R.V-P., S.FdM. and P.V.) and a grant from Junta de Balears-AECC (to G.R., S.FdM. and P.V.).

Compliance with ethical standards

Informed consent For tumor sample collection informed consent was obtained from all individual participants included in the study and the study was approved by the ethical committee (*Comitè d'Ètica de la Investigació-Illes Balears, CEI-IB, Ref. N° 3198/16*).

Conflict of interest The authors declare that they have no conflict of interest.

References

- G.P. Dunn, M.L. Rinne, J. Wykosky, G. Genovese, S.N. Quayle, I.F. Dunn, P.K. Agarwalla, M.G. Chheda, B. Campos, A. Wang, C. Brennan, K.L. Ligon, F. Furnari, W.K. Cavenee, R.A. Depinho, L. Chin, W.C. Hahn, Emerging insights into the molecular and cellular basis of glioblastoma. *Genes Dev* **26**, 756–784 (2012)
- M. Staberg, S.R. Michaelsen, R.D. Rasmussen, M. Villingshøj, H.S. Poulsen, P. Hamerlik, Inhibition of histone deacetylases sensitizes glioblastoma cells to lomustine. *Cell Oncol* **40**, 21–32 (2017)
- D. Matias, J. Balca-Silva, L.G. Dubois, B. Pontes, V.P. Ferrer, L. Rosario, A. do Carmo, J. Echevarria-Lima, A.B. Sarmento-Ribeiro, M.C. Lopes, V. Moura-Neto, Dual treatment with shikonin and temozolomide reduces glioblastoma tumor growth, migration and glial-to-mesenchymal transition. *Cell Oncol* **40**, 247–261 (2017)
- Comprehensive genomic characterization defines human glioblastoma genes and core pathways. *Nature* **455**, 1061–1068 (2008)
- T.F. Cloughesy, W.K. Cavenee, P.S. Mischel, Glioblastoma: From molecular pathology to targeted treatment. *Annu Rev Pathol* **9**, 1–25 (2014)
- M.E. Halatsch, U. Schmidt, J. Behnke-Mursch, A. Unterberg, C.R. Wirtz, Epidermal growth factor receptor inhibition for the treatment of glioblastoma multiforme and other malignant brain tumours. *Cancer Treat Rev* **32**, 74–89 (2006)
- R. Nishikawa, X.D. Ji, R.C. Harmon, C.S. Lazar, G.N. Gill, W.K. Cavenee, H.J. Huang, A mutant epidermal growth factor receptor common in human glioma confers enhanced tumorigenicity. *Proc Natl Acad Sci U S A* **91**, 7727–7731 (1994)
- I.K. Mellinghoff, M.Y. Wang, I. Vivanco, D.A. Haas-Kogan, S. Zhu, E.Q. Dia, K.V. Lu, K. Yoshimoto, J.H. Huang, D.J. Chute, B.L. Riggs, S. Horvath, L.M. Liau, W.K. Cavenee, P.N. Rao, R. Beroukhi, T.C. Peck, J.C. Lee, W.R. Sellers, D. Stokoe, M. Prados, T.F. Cloughesy, C.L. Sawyers, P.S. Mischel, Molecular determinants of the response of glioblastomas to EGFR kinase inhibitors. *N Engl J Med* **353**, 2012–2024 (2005)
- E. Carrasco-Garcia, M. Saceda, S. Grasso, L. Rocamora-Reverte, M. Conde, A. Gomez-Martinez, P. Garcia-Morales, J.A. Ferragut, I. Martinez-Lacaci, Small tyrosine kinase inhibitors interrupt EGFR signaling by interacting with erbB3 and erbB4 in glioblastoma cell lines. *Exp Cell Res* **317**, 1476–1489 (2011)
- G. Ramis, E. Thomas-Moya, S. Fernandez de Mattos, J. Rodriguez, P. Villalonga, EGFR inhibition in glioma cells modulates rho signaling to inhibit cell motility and invasion and cooperates with Temozolomide to reduce cell growth. *PLoS One* **7**, e38770 (2012)
- H.W. Lo, EGFR-targeted therapy in malignant glioma: Novel aspects and mechanisms of drug resistance. *Curr Mol Pharmacol* **3**, 37–52 (2010)
- G. Karpel-Massler, C. R. Wirtz, M.E. Halatsch, Drug combinations enhancing the antineoplastic effects of erlotinib in high-grade glioma. *Recent Pat Anticancer Drug Discov* **6**, 384–394 (2011)
- Q.W. Fan, K.M. Specht, C. Zhang, D.D. Goldenberg, K.M. Shokat, W.A. Weiss, Combinatorial efficacy achieved through two-point blockade within a signaling pathway—a chemical genetic approach. *Cancer Res* **63**, 8930–8938 (2003)
- M.Y. Wang, K.V. Lu, S. Zhu, E.Q. Dia, I. Vivanco, G.M. Shackleford, W.K. Cavenee, I.K. Mellinghoff, T.F. Cloughesy, C.L. Sawyers, P.S. Mischel, Mammalian target of rapamycin inhibition promotes response to epidermal growth factor receptor kinase inhibitors in PTEN-deficient and PTEN-intact glioblastoma cells. *Cancer Res* **66**, 7864–7869 (2006)
- Q.W. Fan, C.K. Cheng, T.P. Nicolaidis, C.S. Hackett, Z.A. Knight, K.M. Shokat, W.A. Weiss, A dual phosphoinositide-3-kinase alpha/mTOR inhibitor cooperates with blockade of epidermal growth factor receptor in PTEN-mutant glioma. *Cancer Res* **67**, 7960–7965 (2007)
- B.M. Burgering, A brief introduction to FOXology. *Oncogene* **27**, 2258–2262 (2008)
- E.W. Lam, R.E. Francis, M. Petkovic, FOXO transcription factors: Key regulators of cell fate. *Biochem Soc Trans* **34**, 722–726 (2006)
- J. Shi, L. Zhang, A. Shen, J. Zhang, Y. Wang, Y. Zhao, L. Zou, Q. Ke, F. He, P. Wang, C. Cheng, G. Shi, Clinical and biological significance of forkhead class box O 3a expression in glioma: Mediation of glioma malignancy by transcriptional regulation of p27kip1. *J Neuro-Oncol* **98**, 57–69 (2010)
- J.Y. Yang, M.C. Hung, A new fork for clinical application: Targeting forkhead transcription factors in cancer. *Clin Cancer Res* **15**, 752–757 (2009)
- T.C. Chou, P. Talalay, Quantitative analysis of dose-effect relationships: The combined effects of multiple drugs or enzyme inhibitors. *Adv Enzym Regul* **22**, 27–55 (1984)
- M.W. Pfaffl, A new mathematical model for relative quantification in real-time RT-PCR. *Nucleic Acids Res* **29**, e45–e45 (2001)
- M.M. Bradford, A rapid and sensitive method for the quantitation of microgram quantities of protein utilizing the principle of protein-dye binding. *Anal Biochem* **72**, 248–254 (1976)
- R.H. Medema, G.J. Kops, J.L. Bos, B.M. Burgering, AFX-like Forkhead transcription factors mediate cell-cycle regulation by Ras and PKB through p27kip1. *Nature* **404**, 782–787 (2000)
- F. Zanella, A. Rosado, B. Garcia, A. Carnero, W. Link, Using multiplexed regulation of luciferase activity and GFP translocation to screen for FOXO modulators. *BMC Cell Biol* **10**, 14 (2009)
- M. Schmidt, S. Fernandez de Mattos, A. van der Horst, R. Klompaker, G.J. Kops, E.W. Lam, B.M. Burgering, R.H. Medema, Cell cycle inhibition by FoxO forkhead transcription factors involves downregulation of cyclin D. *Mol Cell Biol* **22**, 7842–7852 (2002)
- A. Essaghiri, N. Dif, C.Y. Marbehant, P.J. Coffey, J.B. Demoulin, The transcription of FOXO genes is stimulated by FOXO3 and repressed by growth factors. *J Biol Chem* **284**, 10334–10342 (2009)
- U.B. McGovern, R.E. Francis, B. Peck, S.K. Guest, J. Wang, S.S. Myatt, J. Krol, J.M. Kwok, A. Polychronis, R.C. Coombes, E.W. Lam, Gefitinib (Iressa) represses FOXM1 expression via FOXO3a in breast cancer. *Mol Cancer Ther* **8**, 582–591 (2009)
- L. Jiang, X.C. Cao, J.G. Cao, F. Liu, M.F. Quan, X.F. Sheng, K.Q. Ren, Casticin induces ovarian cancer cell apoptosis by repressing FoxM1 through the activation of FOXO3a. *Oncol Lett* **5**, 1605–1610 (2013)
- T.R. Kau, F. Schroeder, S. Ramaswamy, C.L. Wojciechowski, J.J. Zhao, T.M. Roberts, J. Clardy, W.R. Sellers, P.A. Silver, A chemical genetic screen identifies inhibitors of regulated nuclear export of a Forkhead transcription factor in PTEN-deficient tumor cells. *Cancer Cell* **4**, 463–476 (2003)
- S. Fernandez de Mattos, P. Villalonga, J. Clardy, E.W. Lam, FOXO3a mediates the cytotoxic effects of cisplatin in colon cancer cells. *Mol Cancer Ther* **7**, 3237–3246 (2008)
- A. Obrador-Hevia, M. Serra-Sitjar, J. Rodriguez, P. Villalonga, S. Fernandez de Mattos, The tumour suppressor FOXO3 is a key regulator of mantle cell lymphoma proliferation and survival. *Br J Haematol* **156**, 334–345 (2012)
- E. Berry, J.L. Hardt, J. Clardy, J.R. Lurain, J.J. Kim, Induction of apoptosis in endometrial cancer cells by psammaphysene involves FOXO1. *Gynecol Oncol* **112**, 331–336 (2009)
- A.V. Hoekstra, E.C. Sefton, E. Berry, Z. Lu, J. Hardt, E. Marsh, P. Yin, J. Clardy, D. Chakravarti, S. Bulun, J.J. Kim, Progestins activate the AKT pathway in leiomyoma cells and promote survival. *J Clin Endocrinol Metab* **94**, 1768–1774 (2009)
- J. Sangodkar, N.S. Dhawan, H. Melville, V.J. Singh, E. Yuan, H. Rana, S. Izadmehr, C. Farrington, S. Mazhar, S. Katz, T. Albano, P.

- Arnovitz, R. Okrent, M. Ohlmeyer, M. Galsky, D. Burstein, D. Zhang, K. Politi, A. Difeo, G. Narla, Targeting the FOXO1/KLF6 axis regulates EGFR signaling and treatment response. *J Clin Invest* **122**, 2637–2651 (2012)
35. S. Zona, L. Bella, M.J. Burton, G.N. de Moraes, E.W. Lam, FOXM1: An emerging master regulator of DNA damage response and genotoxic agent resistance. *Biochim Biophys Acta* **1839**, 1316–1322 (2014)
 36. M. Liu, B. Dai, S.H. Kang, K. Ban, F.J. Huang, F.F. Lang, K.D. Aldape, T.X. Xie, C.E. Pelloski, K. Xie, R. Sawaya, S. Huang, FoxM1B is overexpressed in human glioblastomas and critically regulates the tumorigenicity of glioma cells. *Cancer Res* **66**, 3593–3602 (2006)
 37. B. Dai, S.H. Kang, W. Gong, M. Liu, K.D. Aldape, R. Sawaya, S. Huang, Aberrant FoxM1B expression increases matrix metalloproteinase-2 transcription and enhances the invasion of glioma cells. *Oncogene* **26**, 6212–6219 (2007)
 38. Y. Zhang, N. Zhang, B. Dai, M. Liu, R. Sawaya, K. Xie, S. Huang, FoxM1B transcriptionally regulates vascular endothelial growth factor expression and promotes the angiogenesis and growth of glioma cells. *Cancer Res* **68**, 8733–8742 (2008)
 39. Y. Lee, K.H. Kim, D.G. Kim, H.J. Cho, Y. Kim, J. Rhee, K. Shin, Y.J. Seo, Y.S. Choi, J.I. Lee, J. Lee, K.M. Joo, D.H. Nam, FoxM1 promotes Stemness and radio-resistance of glioblastoma by regulating the master stem cell regulator Sox2. *PLoS One* **10**, e0137703 (2015)
 40. A.H. Gong, P. Wei, S. Zhang, J. Yao, Y. Yuan, A.D. Zhou, F.F. Lang, A.B. Heimberger, G. Rao, S. Huang, FoxM1 drives a feed-forward STAT3-activation signaling loop that promotes the self-renewal and Tumorigenicity of glioblastoma stem-like cells. *Cancer Res* **75**, 2337–2348 (2015)
 41. K. Joshi, Y. Banasavadi-Siddegowda, X. Mo, S.H. Kim, P. Mao, C. Kig, D. Nardini, R.W. Sobol, L.M. Chow, H.I. Kornblum, R. Waclaw, M. Beullens, I. Nakano, MELK-dependent FOXM1 phosphorylation is essential for proliferation of glioma stem cells. *Stem Cells* **31**, 1051–1063 (2013)
 42. N. Zhang, X. Wu, L. Yang, F. Xiao, H. Zhang, A. Zhou, Z. Huang, S. Huang, FoxM1 inhibition sensitizes resistant glioblastoma cells to temozolomide by downregulating the expression of DNA-repair gene Rad51. *Clin Cancer Res* **18**, 5961–5971 (2012)
 43. N. Zhang, P. Wei, A. Gong, W.T. Chiu, H.T. Lee, H. Colman, H. Huang, J. Xue, M. Liu, Y. Wang, R. Sawaya, K. Xie, W.K. Yung, R.H. Medema, X. He, S. Huang, FoxM1 promotes beta-catenin nuclear localization and controls Wnt target-gene expression and glioma tumorigenesis. *Cancer Cell* **20**, 427–442 (2011)
 44. K. Xu, H.K. Shu, Transcription factor interactions mediate EGF-dependent COX-2 expression. *Mol Cancer Res : MCR* **11**, 875–886 (2013)
 45. J. Krol, R.E. Francis, A. Albergaria, A. Sunter, A. Polychronis, R.C. Coombes, E.W. Lam, The transcription factor FOXO3a is a crucial cellular target of gefitinib (Iressa) in breast cancer cells. *Mol Cancer Ther* **6**, 3169–3179 (2007)
 46. S. Fernandez de Mattos, A. Essafi, I. Soeiro, A.M. Pietersen, K.U. Birkenkamp, C.S. Edwards, A. Martino, B.H. Nelson, J.M. Francis, M.C. Jones, J.J. Brosens, P.J. Coffey, E.W. Lam, FoxO3a and BCR-ABL regulate cyclin D2 transcription through a STAT5/BCL6-dependent mechanism. *Mol Cell Biol* **24**, 10058–10071 (2004)
 47. A. Sunter, S. Fernandez de Mattos, M. Stahl, J.J. Brosens, G. Zoumpoulidou, C.A. Saunders, P.J. Coffey, R.H. Medema, R.C. Coombes, E.W. Lam, FoxO3a transcriptional regulation of Bim controls apoptosis in paclitaxel-treated breast cancer cell lines. *J Biol Chem* **278**, 49795–49805 (2003)
 48. F. Zhao, E.W. Lam, Role of the forkhead transcription factor FOXO-FOXM1 axis in cancer and drug resistance. *Front Med* **6**, 376–380 (2012)
 49. J.E. Allen, G. Kringsfeld, P.A. Mayes, L. Patel, D.T. Dicker, A.S. Patel, N.G. Dolloff, E. Messaris, K.A. Scata, W. Wang, J.Y. Zhou, G.S. Wu, W.S. El-Deiry, Dual inactivation of Akt and ERK by TIC10 signals Foxo3a nuclear translocation, TRAIL gene induction, and potent antitumor effects. *Sci Transl Med* **5**, 171ra117 (2013)
 50. J. Sunayama, A. Sato, K. Matsuda, K. Tachibana, E. Watanabe, S. Seino, K. Suzuki, Y. Narita, S. Shibui, K. Sakurada, T. Kayama, A. Tomiyama, C. Kitanaka, FoxO3a functions as a key integrator of cellular signals that control glioblastoma stem-like cell differentiation and tumorigenicity. *Stem Cells* **29**, 1327–1337 (2011)
 51. Z. Qian, L. Ren, D. Wu, X. Yang, Z. Zhou, Q. Nie, G. Jiang, S. Xue, W. Weng, Y. Qiu, Y. Lin, Overexpression of FoxO3a is associated with glioblastoma progression and predicts poor patient prognosis. *Int J Cancer* **140**, 2792–2804 (2017)
 52. F.C. Schroeder, T.R. Kau, P.A. Silver, J. Clardy, The psammaplysenes, specific inhibitors of FOXO1a nuclear export. *J Nat Prod* **68**, 574–576 (2005)
 53. S.H. Curry, R.B. Stewart, P.K. Springer, J.E. Pope, Plasma-trifluoperazine concentrations during high dose therapy. *Lancet* **1**, 395–396 (1981)
 54. B.M. Cohen, J.F. Lipinski, C. Waternaux, A fixed dose study of the plasma concentration and clinical effects of thioridazine and its major metabolites. *Psychopharmacology* **97**, 481–488 (1989)
 55. I. Gil-Ad, B. Shtatif, Y. Levkovitz, M. Dayag, E. Zeldich, A. Weizman, Characterization of phenothiazine-induced apoptosis in neuroblastoma and glioma cell lines: Clinical relevance and possible application for brain-derived tumors. *J Mol Neurosci : MN* **22**, 189–198 (2004)
 56. H.W. Cheng, Y.H. Liang, Y.L. Kuo, C.P. Chuu, C.Y. Lin, M.H. Lee, A.T. Wu, C.T. Yeh, E.I. Chen, J. Whang-Peng, C.L. Su, C.Y. Huang, Identification of thioridazine, an antipsychotic drug, as an anti-glioblastoma and anticancer stem cell agent using public gene expression data. *Cell Death Dis* **6**, e1753 (2015)
 57. S.Y. Shin, K.S. Lee, Y.K. Choi, H.J. Lim, H.G. Lee, Y. Lim, Y.H. Lee, The antipsychotic agent chlorpromazine induces autophagic cell death by inhibiting the Akt/mTOR pathway in human U-87MG glioma cells. *Carcinogenesis* **34**, 2080–2089 (2013)
 58. J.K. Lee, D.H. Nam, J. Lee, Repurposing antipsychotics as glioblastoma therapeutics: Potentials and challenges. *Oncol Lett* **11**, 1281–1286 (2016)
 59. J. Colomer, A.A. Schmitt, E.J. Toone, A.R. Means, Identification and inhibitory properties of a novel ca(2+)/calmodulin antagonist. *Biochemistry* **49**, 4244–4254 (2010)
 60. F. Zanella, A. Rosado, B. Garcia, A. Carnero, W. Link, Chemical genetic analysis of FOXO nuclear-cytoplasmic shuttling by using image-based cell screening. *Chembiochem* **9**, 2229–2237 (2008)
 61. J. Li, S. Zhu, D. Kozono, K. Ng, D. Futalan, Y. Shen, J.C. Akers, T. Steed, D. Kushwaha, M. Schlabach, B.S. Carter, C.H. Kwon, F. Furnari, W. Cavenee, S. Elledge, C.C. Chen, Genome-wide shRNA screen revealed integrated mitogenic signaling between dopamine receptor D2 (DRD2) and epidermal growth factor receptor (EGFR) in glioblastoma. *Oncotarget* **5**, 882–893 (2014)

Publisher's note Springer Nature remains neutral with regard to jurisdictional claims in published maps and institutional affiliations.